Research Article

Open Access

Ifty Ahmed*, S. S. Shaharuddin, N. Sharmin, D. Furniss, and C. Rudd

Core/Clad Phosphate Glass Fibres Containing Iron and/or Titanium

Abstract: Phosphate glasses are novel amorphous biomaterials due to their fully resorbable characteristics, with controllable degradation profiles. In this study, phosphate glasses containing titanium and/or iron were identified to exhibit sufficiently matched thermal properties (*glass transition temperature, thermal expansion coefficient and viscosity*) which enabled successful co-extrusion of glass billets to form a core/clad preform. The cladding composition for the core/clad preforms were also reversed. Fe clad and Ti clad fibres were successfully drawn with an average diameter of between 30~50 μm. The average cladding annular thickness was estimated to be less than 2 μm. Annealed core/clad fibres were degraded in PBS for a period of 27 days. The strength of the Fe clad fibres appeared to increase from 303 ± 73 MPa to 386 ± 45 MPa after nearly 2 weeks in the dissolution medium (phosphate buffered solution) before decreasing by day 27. The strength of the Ti clad fibres revealed an increase from 236 ± 53 MPa to 295 ± 61 MPa when compared at week 3. The tensile modulus measured for both core/clad fibres ranged between 51 GPa to 60 GPa. During the dissolution study, Fe clad fibres showed a peeling mechanism compared to the Ti clad fibres.

Keywords: core/clad phosphate glass fibres, mechanical properties, degradation, thermal properties

*Corresponding Author: Ifty Ahmed: Faculty of Engineering, Division of Materials, Mechanics and Structures, University of Nottingham, NG7 2RD, E-mail: ifty.ahmed@nottingham.ac.uk
S. S. Shaharuddin: Department of Manufacturing and Materials Engineering, Kuliyyah of Engineering, International Islamic University Malaysia, Malaysia.
N. Sharmin: Faculty of Engineering, Division of Materials, Mechanics and Structures, University of Nottingham, NG7 2RD.
D. Furniss: Faculty of Engineering, Division of Materials, Mechanics and Structures, University of Nottingham, NG7 2RD.
C. Rudd: Faculty of Engineering, Division of Materials, Mechanics and Structures, University of Nottingham, NG7 2RD.

1 Introduction

Phosphate glasses (PG) are novel materials as they offer a wide range of degradation profiles which can be tailored to suit the end application [1]. Interest in these materials stems back to the 1950's when Van Wazer first presented the foundations and understanding of the nature of PGs. Kordes *et al.* were also investigating PGs about the same time and noted some "anamolous trends" which they suggested showed a compositional dependence [45].

In the last 25 years, interests in PG as potential materials for structural reinforcement in resorbable matrices have grown significantly. Initial studies on PGs mostly focused on binary and ternary glass systems such as P_2O_5-CaO [2] and P_2O_5-CaO-Na_2O [3–6], whereby the phosphate contents were fixed at 45, 50 and 55 mol% and the CaO:Na_2O ratios were varied. The benefits of utilising PGs for biomedical use can be seen in their compositions, as they contain elements that are present in the body and as such should be biocompatible [7]. In addition, it has been found that introducing relatively low amounts of Fe_2O_3 or TiO_2 to PGs was successful for cellular attachment and proliferation [8–10]. The success of these *in vitro* studies was linked to their improved durability due to addition of these oxides.

PGs of various compositions have been successfully fiberised via the melt drawn method [2, 11–13]. These PGs have been investigated for use as fibrous reinforcement to improve the mechanical properties of resorbable polymers (*e.g.* PLA and PCL) for orthopaedic applications such as bone fracture fixation devices [14]. For load bearing applications, implants/devices should ideally have mechanical properties slightly superior to or similar to that of cortical bone [15]. During degradation, these composites should be able to allow for stress transfer to the healing bone. It has also been suggested that the mechanical properties of these devices should be maintained for a period of 8-12 weeks to allow for bone healing to occur depending on the site of implantation and age of the patient [16].

It has been reported that glasses with similar glass transition temperatures and viscosity/temperature profiles can be successfully co-extruded to produce core/clad

Table 1: Glass nominal batch compositions in mol%, including including their drying, melting and casting temperature used during glass preparation.

Glass code	P_2O_5 /mol%	CaO /mol%	Na_2O /mol%	MgO /mol%	Fe_2O_3 /mol%	TiO_2 /mol%	Drying temperature /°C	Melting temperature /°C	Melting time /hr
P50 Fe5	50	16	5	24	5	-	400	1100	1.5
P45 Ti5	45	16	10	24	-	5	400	1300	3.0

Table 2: Glass codes for core/clad performs

Core/clad code	Core Glass code	Clad Glass code
Core/clad Ti5_ Fe5	P45 Ti5	P50 Fe5
Core/clad Fe5_ Ti5	P50 Fe5	P45 Ti5

preforms [17, 18], from which fibres can then be drawn using a preform drawn method. The development of structured fibres (*i.e.* with different core/clad properties) is common for optical fibres as a method to control refractive indices. However, manufacture of core/clad glasses for bioresorbable PGs has not been done before and could allow for further potential control over their properties which have not previously been achieved. For example it was hypothesised that hollow tubes could be formed ex vivo or *in vivo* and *in situ* upon degradation over time which could potentially be used as guides to direct cell growth [19, 20]. Several studies have shown that phosphate glasses can be incorporated with various therapeutic ions such as copper [12, 21], zinc and silver [22–25] to impart antimicrobial properties upon degradation and calcium is known to be an important element for wound healing [26]. Therefore it can also be envisaged that a core/clad glass system incorporating any of these therapeutic ions in the core or cladding of the glass could allow for a sequence of controlled antibacterial and/or wound healing activity. In addition, these novel core/clad glass structures could also potentially enable controlled ion release for pharmaceutical applications (*i.e.* in amorphous drug formulations).

The initial aim of the current study was to investigate the feasibility of manufacturing co-extruded (core-clad) phosphate based glass combinations, with the aim to design core-clad structures with varying degradation profiles. Individual PG formulations for core and clad glass combinations were selected based upon matching thermal properties. The composition of the core and clad glasses were also reversed to compare their effect on mechanical strength of the fibres formed from these core/clad combinations. Their surface morphology and mechanical prop-

erty retention during dissolution studies in phosphate buffered saline (PBS) were also evaluated.

2 Materials and Methodology

2.1 Glass preparation

Two glass compositions with comparable thermal properties were prepared using sodium dihydrogen phosphate (NaH_2PO_4, ≥ 99%), calcium hydrogen phosphate ($CaHPO_4$, 98-105%), phosphorous pentoxide (P_2O_5, > 98%), iron (III)-phosphate dehydrate ($FePO_4 \cdot 2H_2O$, ≥ 26%) and magnesium phosphate dibasic trihydrate ($MgHPO_4 \cdot 3H_2O$, ≥ 98%) all obtained from Sigma Aldrich, UK. The titanium (IV) oxide (TiO_2, ≥ 99.5%) was obtained from Riedel-de Haen, Germany. See Table 1 for the respective glass codes for the glass compositions (mol%) produced.

The precursors were weighed and transferred to a 100 ml volume Pt/5% Au crucible (Birmingham Metal Company, U.K.). The samples were first dehydrated for 30 min at 350°C followed by melting in a furnace at the corresponding temperatures and time as given in Table 1.

The glass melt was then poured onto a steel plate and left to cool to room temperature. Once cooled, the as-quenched glasses were crushed into powders and sieved to obtain glass particles with a diameter in the range of 106 and 53 microns, which were used for differential scanning calorimetry analysis.

Glasses were also re-melted and cast into a pre-heated cylindrical graphite mould to produce 4 mm diameter sample rods for viscosity/temperature and thermal expansion measurements. On cooling, the glass rods were removed
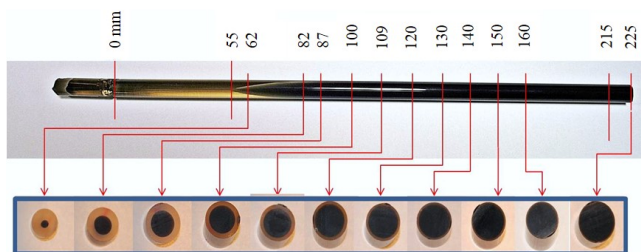
Figure 1: Example of the cross-sections of one of the extruded core/clad preforms used to obtain core/clad fibres via preform fibre drawing.

Figure 2: Fibre production from extruded core/clad preforms. Fibres were drawn with diameters ranging from 30-50 μm.

and annealed in a furnace (Carbolite, UK) by heating at a rate of 3°C min^{-1} to T$_g$ + 10°C holding for 1 hour [16] and then cooling to room temperature at approximately 2°C min^{-1}. The 4 mm diameter annealed glass rods were cut accordingly to specific height suitable for each test (*i.e.* 3 mm for viscosity/temperature and 7 mm for thermal expansion measurements) using a diamond edge circular saw (Isomet low speed saw, Buehler, UK). The top and bottom of the cylindrical samples for viscosity/temperature and thermal expansion measurements were ground lightly with 1000 grit SiC paper using oil as a lubricant to ensure that they were flat. The surfaces of the cylindrical samples were then rinsed using reagent grade acetone and air dried.

For the extrusion process, individual glass billets measuring 28 mm in diameter were cast into a preheated cylindrical graphite mould with inner diameters of 28 mm.

2.2 Thermal analysis

The thermal properties of the glasses were determined via differential scanning calorimetry analysis (TA Instruments Q10, U.K). Approximately 30 mg of the glass powders (particle size in the range of 106 and 53 microns) were tested to determine the T$_g$ in which samples (n = 3) were heated from room temperature at 20°C min^{-1} in flowing argon gas. The T$_g$ was extrapolated from the onset of change in the endothermic reaction of the heat flow.

The viscosity/temperature measurements were conducted utilising a parallel plate method via a thermomechanical analyser (Perkin Elmer Thermomechanical Analyser TMA 7, UK). For this methodology small glass rods with diameters of approximately 4 mm and average heights of 2.6 mm were used. The samples were sandwiched between two stainless steel parallel plates, where the top plate was fitted to the TMA silica sample probe. A force of 170 mN was applied to the top plate via the silica sample probe. During the experiments helium was passed through the sample chamber at 20 ml min^{-1}. The TMA was calibrated using standard materials (indium and aluminium). The temperature was increased initially from room temperature to T$_g$ at a rate of 40°C min^{-1}, held isothermally at T$_g$ for 3 minutes and then to T$_g$ + 120°C at 5°C min^{-1}. The viscosity/temperature relationship was compiled by measuring the deformation rate with temperature using Gent's equation [27].

The thermal expansion coefficient (α) was measured using a thermo-mechanical analyser, TMA (TA Instruments SDT Q400, UK). Three repeat samples of approximately 4 mm in diameter and 7 mm in height were tested from room temperature at a heating rate of 5°C min^{-1} with an applied load of 50 mN. All measurements were conducted in an argon atmosphere flowing at a rate of 70 ml min^{-1}. The measured thermal expansion coefficient was taken as average between 50°C to glass transition temperature of the respective glasses.

2.3 Extrusion and fibre drawing of core/clad preforms

Individual glass billets were prepared via casting in graphite mould as mentioned in Section 1.1. Manufacture via extrusion of the glass billet from approximately 28 mm diameter to a 9 mm diameter preform was performed using an in-house designed extruder.

The core/clad preforms were prepared via co-extrusion of P50 Fe5 and P45 Ti5 billets. The core and clad glass billets were cut using a diamond edge circular saw (Isomet low speed saw, Buehler, UK) at both ends to achieve an equal height of 20 mm. The glass billets were then lightly polished with 1000 grit SiC paper and cleaned with acetone (Sigma Aldrich, UK, ≥ 99.5%). These core and clad billets were then loaded into the extruder barrel and abutted such that, in the vertical position, the cladding glass was located underneath the core glass in the barrel and closer to the die. The core and clad preforms were co-extruded by heating these bulk glass billets to an extrusion temperature corresponding to log viscosity 10^8 Pa s,
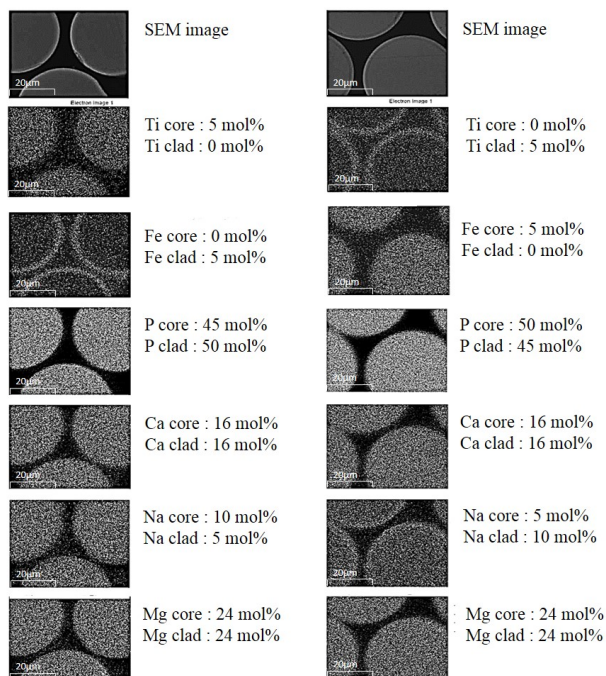
Figure 3: SEM images as well as elemental distribution for (a) core/clad Ti5_ Fe5 and (b) core/clad Fe5_ Ti5.

where the material would be sufficiently soft to allow it to be forced through a die structure via a hydraulic punch into a free space to form an extrudate. The core and clad glasses were also reversed and their respective codes can be found in Table 2. Similar extrusion process was also performed to produce monolithic P45 Ti5 and P50 Fe5 preforms.

Fibre drawing of the individual preforms and core/clad preform was performed utilising a specially designed and built fibre drawing tower (Controls Interface Ltd). Nitrogen (BOC, UK, ≥ 99%) gas was supplied to the top and bottom of the furnace cavity in order to maintain an inert gas atmosphere during fibre drawing.

2.4 SEM/EDX analysis

SEM/EDX analysis was performed for core/clad fibres with diameters in the range of 39-45 μm using the elemental mapping option via the Oxford Instruments INCA SEM/EDX system. The cladding annular thickness (*i.e.* radial distance between the core and clad interface and the outer fibre surface) and the diameters of the fibres were also determined for the core-clad fibres (see Figure 3).

2.5 X-Ray Diffraction (XRD)

To investigate the amorphous nature of the fibres produced, the fibres were ground into fine powder using an agate pestle and mortar. The X-ray diffraction spectra were obtained using a Bruker D500 X-ray diffractometer at room temperature and ambient atmosphere with Ni-filtered Cu Ka radiation, generated at 40 kV and 40 mA. Scans were performed with a step size of 0.02° and a step time of 0.5 s over an angular range 2θ from 15° to 100°.Two repeats were performed for each sample.

2.6 Single Fibre Filament Test (SFTT)

The SFTT was performed using a LEX810 Tensile Tester (UK) at room temperature with a load capacity of 0.2 N and a speed of 0.017 mm·min^{-1}. Statistical analysis was carried out using GraphPad Prism for Windows (GraphPad, Software Inc, USA) in which the significance was detected at a 0.05 level.In addition Weibull statistical analysis of the glass fibres was conducted via Minitab 15 (Minitab Inc, USA).

Essentially, 20 fibres ranging between 39-45 μm in diameter were individually mounted onto plastic tabs with a 25 mm gauge length test set-up. The ends of each fibre were bonded to the plastic tab with an epoxy adhesive, Dymax 3099 (Dymax, Europe) and the epoxy was cured using UV light. The fibre specimen was lifted by vacuum suction which gripped the tabs bonded to the ends of the fibre and was positioned in front of a laser scan micrometer, LSM 6200 (Mitutoyo, Japan) in order to directly measure the individual diameter of the fibre prior to testing. The laser scan micrometer was calibrated with glass fibres of various diameters and the error on diameter measurements was approximately ± 0.3 μm.

2.7 Fibre Degradation Test

The as drawn fibres were cut into length of 70 mm and placed on aluminium foil in a furnace (Carbolite, UK). The annealing schedule was to heat the fibres from ambient temperature to T_g + 10°C for 1 hour at 3°C·min^{-1} [14] and then cool to room temperature at 2°C·min^{-1}. The annealed fibres were then cut into an average length of 50 mm with a mass of 300 mg and were placed into individual glass vials containing 30 ml of PBS solution. At each time point, the fibres were removed and placed on to a weighing boat. They were then placed in a vacuum drying oven at 50°C for 24 hour before being prepared for tensile test measure-

Table 3: Thermal properties (T_g, T_x, α and approximated temperature at melt viscosity of 8 Pa s) ofP45 Ti5 and P50 Fe5.

Glass code	T_g /°C	T_x /°C	α /$\times 10^{-6}$°C^{-1}	Approximated extrusion temperature at viscosity of 8 Pa s /°C
P45 Ti5	491.6 ±1.2	585.9±1.5	12.3± 0.3	525
P50 Fe5	493.4 ±0.8	594.0±0.3	11.1± 0.1	531

ments. Fresh PBS solution was replaced at time points 1, 3 and 6 days for the first week and at 2 time points per week for the rest of the dissolution period of 54 days.

3 Results

3.1 Thermal analysis

Table 3 shows the glass transition temperature (T_g), onset of crystallisation temperature (T_x), thermal expansion coefficient (α) and approximated extrusion temperature for P50 Fe5 and P45 Ti5 glass formulations. There was no significant difference between the T_g values of P50 Fe5 and P45 Ti5 glass formulations. The thermal stability (defined as the difference between T_g and T_x) *i.e.* the processing window of the glasses were approximately 94°C and 100°C for P45 Ti5 and P50 Fe5 glass formulations, respectively. The thermal expansion coefficient measured was found to be only slightly higher for P45 Ti5 compared to P50 Fe5. Both glasses exhibited approximately similar viscosity of 8 Pa s at 525°C and 531°C.

3.2 Preform extrusions and fibre drawing

The estimated extrusion temperatures for the individual core and clad glasses provided a starting point and during the extrusion process both temperature and pressure was adjusted to obtain a constant extrusion rate of 1 mm·min^{-1}. Several core/clad preforms were produced during this study. All core/clad preforms produced showed slightly different distributions of the core and clad dimensions. Figure 1 shows a representative distribution of the core and clad dimensions achieved for the core/clad preforms manufactured. The first part of the preform to exit the extruder was marked and designated as 0 mm. The preform was initially sliced at approximately 7 mm and 20 mm along the length of the preform and then at constant 10 mm intervals. The preform was thus divided into three distinct phases. The first phase with zero (core/clad) ratio occurred from 0 to 55 mm. In the second phase, the core increased

along the length of the preform from 55 mm to 109 mm. In the final third phase, the thickness of the sliced preform at 109 mm was approximately 1 mm and beyond at this point, the cladding structure was not clearly visible and was expected to have a more gradual change in thickness until 225 mm. Based on the varying thickness of the core and clad, it was decided that fibre drawing of the preform would be initiated at the latter end of the preform in order to obtain an even distribution of the cladding achieved.

The extruded core/clad preforms were successfully drawn into fibres with diameters ranging from 30-50 μm (see Figure 2). Evidence of the cladding structure as well as the elemental mapping for P, Ca, Na, Mg, Fe and Ti for the core/clad fibres can clearly be seen in Figures 3 and 4a. The average cladding annular thickness for the core/clad fibres were estimated to be less than 2 μm.

3.3 XRD analysis

It was apparent from the XRD analyses (see Figure 4b) performed for the core/clad glasses investigated that they were amorphous as evident from the "amorphous hump" seen between 15° and 40° (2θ) [28].

3.4 Single Fibre Filament Test (SFTT)

All the fibres were heat treated prior to being degraded in PBS. The mechanical properties of the annealed core/clad fibres are shown in Table 4 .The strength of core/clad P45/P50 fibres appeared to be statistically significant ($P < 0.001$) higher compared to P50/P45 fibres. Whilst, the modulus of both core/clads did not show any statistically significant difference ($P > 0.05$).

During the dissolution study, the strength of core/clad P45/P50 appeared to increase between day 0 and day 13 and then decreased from day 13 to day 27 which was found to be statistically significant ($P < 0.001$). Similar comparisons were made between day 0 and day 13 for core/cladP50/P45. The results showed that there was no statistically significant ($P > 0.05$) difference in strength during the initial two weeks of the degradation period (see

Table 4: The strength and modulus of annealed core/clad Ti5_ Fe5 and core/clad Fe5_ Ti5 fibres

Core/clad code	Tensile strength / MPa	Tensile modulus / GPa
Core/clad Ti5_Fe5	302.9±73.4	56.1±5.1
Core/clad Fe5_Ti5	235.5±52.6	58.2±3.8

(a)

(b)

Figure 4: (a) Fibre diameters obtained including estimated cladding thickness for core/cladTi5_Fe5 and core/clad Fe5_Ti5 fibres. (b) XRD plots for core/clad fibres P45/P50 and P50/P45

(a)

(b)

Figure 5: (a) Change in tensile strength for core /clad Ti5_Fe5 and core/clad Fe5_Ti5 fibres (with their respective SEM images above) after degradation in PBS at 37°C measured at various time points from day 0 to day 27. (b) Change in tensile modulus for core/clad Ti5_Fe5 and core/clad Fe5_Ti5 fibres after degradation in PBS at 37°C measured at various time points from day 0 to day 27.
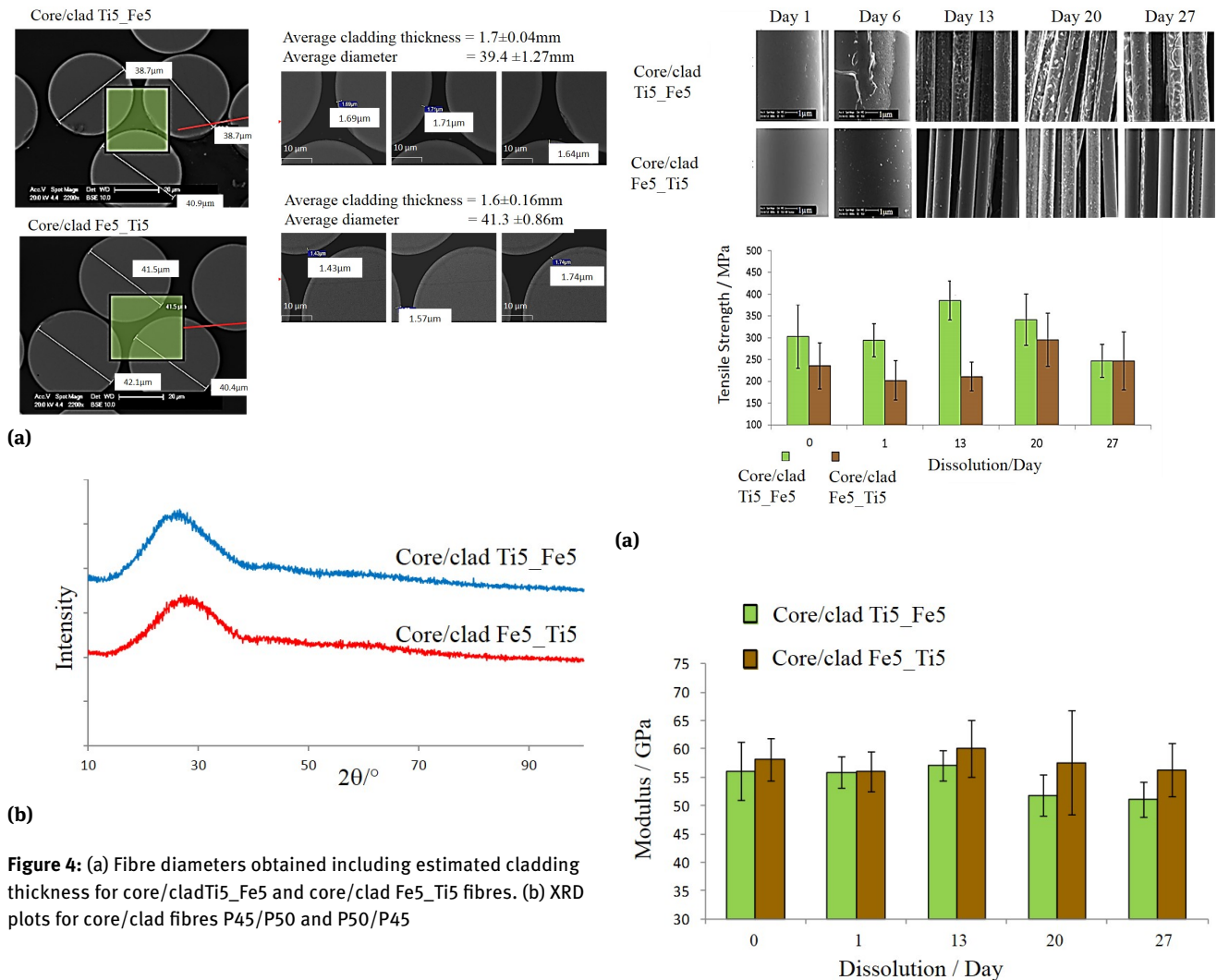
Figure 5a). The strength of core/cladP50/P45 increased when compared between day 1 to day 20. And between day 20 and 27, the strength decreased to 247 ± 667 MPa. The modulus of core/clad P45/P50 as shown in Figure 5b showed a decreasing trend based on the comparisons made between day 0 and day 27. Whilst, the modulus of core/clad P50/P45 did not show any statistically significant (P > 0.05) difference when compared between day 0 and day 27. The modulus of P50/P45 was maintained in

the range of 56 GPa – 60 GPa over 27 days. In addition, no significant reduction in diameter was observed for these core/clad fibres (see Figure 6).

The SEM images of the degraded fibres revealed that the surface of the degraded Fe clad P50 Fe5 (from core/clad P45/P50) showed a peeling effect from day 6. However,
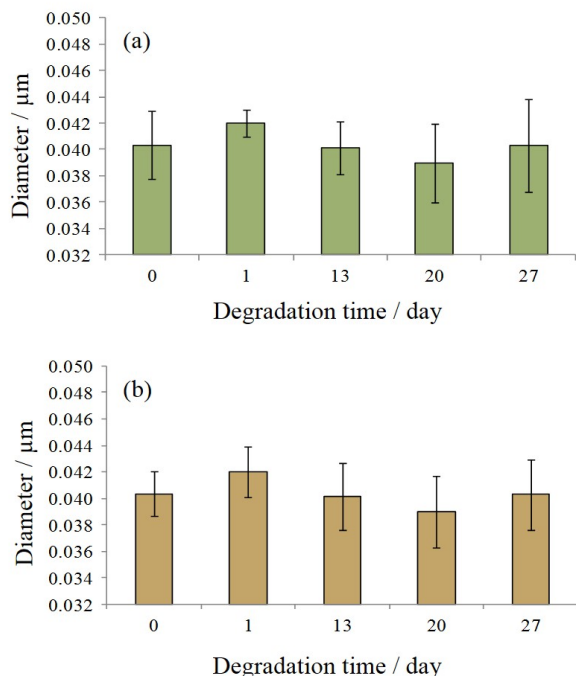
core/cladP50/P45fibres with Ti cladding (P45 Ti5) did not exhibit any peeling effect at all during the 27 day dissolution period. In order to confirm the surface morphology of these core/clads, fibres were also drawn from the monolithic preform compositions of P45 Ti5 and P50 Fe5 fibres which were also degraded using the same dissolution protocol. The surface morphology of degraded P45 Ti5 fibres appeared to be smooth and were found to be comparable as those found in core/clad P50/P45(clad: P45 Ti5) (see Figure 7a). Similar surface comparisons were also made for P50 Fe5 and core/clad P45/P50 (clad: P50 Ti5) fibres. Cracks and peeling effects were also observed for P50 Fe5 fibres as shown in Figure 7b. This confirmed that the cladding composition of P45 Ti5 and P50 Fe5 had undergone different effects of surface deterioration in PBS.

The SEM image of core/clad P45/P50 and core/clad P50/P45 (see Figure 5a) at day 13 and day 27 showed that the structural integrity of the fibres was maintained.

4 Discussion

The main purpose of this study was to investigate the feasibility of manufacturing co-extruded (core-clad) phosphate based glass combinations. Fibres were drawn from core/clad preforms and their mechanical properties were compared. The mechanical as well as surface morphologies of core/cladP45/P50 and core/clad P50/P45 which were also reversed were then observed for their dissolution profiles in PBS over a 27 day period.

Figure 6: The change in fibre diameter for (a) core/clad Ti5_Fe5and (b) core/clad Fe5_Ti5fibres after degradation in PBS at 37°C measured at various time points from day 0 to day 27.
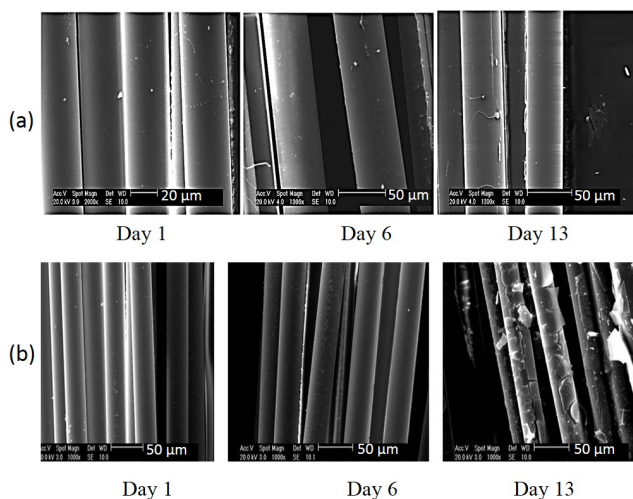

Figure 7: (a) Surface morphology of degraded P45 Ti5 fibres at day 1, 6 and 13. And (b) Surface morphology of degraded P50 Fe5 fibres at day 1, 6 and 13.

Thermal properties

Thermal properties of the P50Fe5 and P45Ti5 glasses as presented in Table 3 showed that both glasses shared similar T_g (~490°C) profiles. It has been reported previously by Savage *et al.* [18] that a close match in T_g between the core and the cladding glasses is of great benefit which allows them to be worked together during the extrusion process. They also suggested that a large difference in softening points could lead to one glass of a core and cladding pair being very difficult to work due to increasing viscosity whilst the other would be too soft [18]. The thermal stability (*i.e.* processing window) given by the difference between T_g and onset of crystallisation (T_x) for the individual glasses used to make up the core/clads were in the range of 94°C - 100°C. The thermal stability of the glasses investigated indicated the resilience of these glasses against crystallisation upon reheating of the preform. Therefore, it

was expected that with the right drawing rate and temperature, these preforms may be fiberised without crystallisation. The amorphous nature of the core/clad fibres was confirmed via XRD analysis (see Figure 4b).

Theoretically, the greater the thermal expansion mismatch between the core and the clad glasses, the greater the stresses produced in the glass during preform fabrication and fibre drawing which may lead to preform cracking and fibre breakage. However, Mairaj *et al.* [29] suggested that the match between an expansion coefficient within $0.8 \times 10^{-6}°C^{-1}$ was suitable for extrusion and a tolerable limit of up to $\alpha = \pm 1.5 \times 10^{-6}°C^{-1}$ was expected. The maximum thermal expansion coefficient difference of both the core and clad glasses was approximately $1.2 \times 10^{-6}°C^{-1}$. Therefore, it was hypothesised that it would be possible to pull fibres from these P50 Fe5 and P45 Ti5 core-clad system preforms without the preform cracking or fibre breakage due to the good match between the thermal expansion coefficient values.

Extrusion and fibre drawing

The extrusion temperature for the performs was suggested to be in the range between 10^6 Pa s < log η < 10^8 Pa s [29]. The difference in viscosity of the core and clad during extrusion can affect the ratio of the core and clad. For instance, if the clad glass becomes less viscous at the extrusion temperature, then it would be expected that more of the cladding glass would be extruded before merging of the core and clad. Therefore the thickness of cladding for the core would be thinner. In addition Lee and Taylor [30] highlighted that a core glass that was considerably softer and less viscous than the cladding glass during extrusion, could lead to a situation where the core might flow directly through the cladding glass. The cladding distribution along the length of the preform is readily explained by the behaviour of the glass billets in the extruder [18]. At first only cladding was extruded as it was placed nearest to the die. As the extrusion progressed it became more difficult for the cladding glass melt to be extruded as it effectively becomes trapped in the corners of the barrel close to the extruder die, and so the core glass melt pushes through the die and gradually thickens as observed in Figure 1. A good degree of confidence can be given to the measured log viscosity/temperature plots since all the core/clads were extruded within close range of the estimated extrusion temperature at log viscosity 8 Pa s (see Table 3). The feasibility of drawing these core/clad fibres may have been aided by the fact that the viscosity of the glasses was almost similar within the range of fibre drawing temperature.

Mechanical properties of core/clad fibres

In general, the manufacture of core and clad preforms and fibres is associated with generation of residual stresses owing to the differences in their thermal expansion coefficients. These residual stresses are generated during the cooling of both preform and fibre to room temperature. Furthermore, mechanically induced stress also occurs during stretching of the preform or drawing of the fibre due to radial variation of the viscoelastic properties [31]. Theoretically, the mechanical integrity and strength of the fibre increased by avoiding tensile stresses in the core/clad structure, whilst an overall compressive stress is beneficial [32]. In addition, it is known that fibre strength is often controlled by sub microscopic damage to the surface of the fibre as well as slight imperfections and/or particulate contaminants on the surface [33–35]. Polishing and etching may help to improve the condition of the preform surface since both methods could remove coarser and finer defects respectively [36, 37]. Furthermore, core/clad compositions could also possess possible defects at the interphase to include bubbles and stress cracking [38]. The glass billets were prepared from casting in graphite moulds and prior to the extrusion process the ends of the billets were cut with a diamond saw, lightly polished with 1000 grit SiC paper and then cleaned with acetone. The polishing procedure could have caused some damage or possibly left debris on the surface. These defects could have trapped gas (as nitrogen gas was passed through the extruder) to cause imperfections such as bubbles in the core and clad interphase [18].

Mechanical properties of partially degraded core/clad fibres

Unlike tensile strength, the tensile modulus represents an intrinsic property of the material. The modulus obtained for the core/clad fibres did not show any statistically significant difference (P > 0.05) during immersion in PBS and was maintained in the range of 51 GPa – 60 GPa over 27 days. The modulus of PG containing Fe_2O_3 or TiO_2 have also been previously reported with values of 52 GPa [39] and 30-35 GPa respectively [40]. The strength of both annealed core/clad fibres was found to be in the range of 303-236 MPa.

Surface morphology of the core/clad P45/P50 and core/clad P50/P45 fibres showed a different mode of degradation as seen in Figures 7a and 7b. For the Fe clad core/clad P45/P50, cracks and thin shells of skins were seen to be peeling off the outer layer at day 6 and revealed a surface layer with small pits. This surface morphology was suggested to be the result of formation of a hydrated layer. These fibres had been wrapped in aluminium foil and then annealed in air. A study by Hayden *et al.* [41] revealed that during annealing in the oven, water vapour in the ambient air can chemically attack phosphate glass surfaces, cleaving P-O-P chains and leaving behind shorter chains that terminate in hydroxyl group. Hayden *et al.* [41] also found that greater content of OH groups existed at the surface therefore creating a pre-hydrated layer. Abou Neel *et al.* [20] reported similar formation of cracks on the surface of degraded fibres and suggested that they were due to the formation of a hydrated layer at the initial stages of the degradation.

The strength of the degraded fibres appeared to peak at day 13 and the corresponding surface morphology indicated a peeling of the outermost layer (see Figure 7b). Cozien-Cazuc [42] and Colaizzi *et al.* [43] attributed the increase in strength of the fibre was due to the progressive removal of the outer tensile layer with its inherent flaws. By day 27, the cracking and peeling effects became much more obvious and the pits had grown larger which ultimately caused the observed decrease in the strength of the fibres [44]. The decrease in strength of Fe5 clad fibres were also accompanied by a decrease in modulus. A repeat of the dissolution study was performed using annealed monolithic P50 Fe5 fibres. The result showed similar surface morphology as the Fe clad core/clad P45/P50 during degradation.

The Ti clad P50/P45 fibres also revealed similar profiles in strength. However, in comparison to the core/clad P45/P50, the increase in strength was slightly delayed at day 20. Morphological examination of the fibres revealed that the surface of the fibre remained intact compared to the Fe clad fibres of core/cladP45/P50. Thus it was inferred that the Ti clad fibre was more durable than the Fe clad fibre and this was confirmed by a repeated experiment of monolithic P45 Ti5 fibre. Thus, it was postulated that the process of etching to remove surface defects which can act as stress concentrators was slower and hence delayed the increase in strength for these fibres.

The formation of a hollow tube was not observed by day 27 as these Fe and Ti containing glasses were fairly durable. In comparison between these two core/clads, it was suggested that producing a thicker Ti cladding over a thicker fibre may have stood a better chance of creating a hollow tube formation as the surface morphology was found to be unchanged during the dissolution period. Or alternatively, using a less durable binary or ternary glass formulation as core could have enabled the formation of a hollow tube.

The limit for matching these phosphate glasses in terms of viscosity/temperature profile and thermal properties such as T_g, thermal expansion coefficient for producing core/clad preforms has not been reported before. This study highlighted the successful feasibility and proof-of-concept for manufacturing core/clad preforms and fibres from PG compositions. Follow-on studies will investigate alternate slow and fast resorbing formulations and their respective ion release profiles.

5 Conclusions

The thermal properties of phosphate glasses containing 5 mol% TiO_2 and/or Fe_2O_3 were investigated. These glasses were found to have sufficient matching thermal properties (T_g, thermal expansion coefficient and viscosity) which enabled the successful co-extrusion and fibre drawing of core-clad 'preforms' and core-clad 'fibres'. The processing window or thermal stability of these glasses (in the range of 94-100°C) also contributed to the feasibility of drawing the core/clad and individual monolithic preforms into fibres. The tensile strength of the annealed fibres prior to degradation in PBS was 303 MPa and 236 MPa for core/clad P45/P50 and P50/P45. After 27 days the strength of both core/clads reached an average of 246 MPa. The tensile modulus of both core/clads was in the range of 51-60 GPa. Comparisons made on the surface morphology of the core/clads showed distinct patterns in which the Fe clad P45/P50 underwent a peeling effect compared to the Ti clad P50/P45 which relatively remained intact. Similar degradation patterns were also observed for the monolithic PG fibres containing either Fe or Ti. It is thus envisaged that a core/clad glass system incorporating alternate/varying therapeutic ions either in the core or cladding of the glass could allow for a sequence of controlled ion release activity for varying biomedical applications.

References

[1] Knowles J.C., Phosphate Based Glasses for Biomedical Applications, J. Mater. Chem. 2003, 13, 2395-2401

[2] Ahmed I., Parsons A.J., Palmer G., Knowles J.C., Walker G.S., Rudd C.D., Weight Loss, Ion Release and Initial Mechanical Properties of a Binary Calcium Phosphate Glass Fiber/PCL Composite, Acta Biomater. 2008, 4, 1307-1314

[3] Ahmed I., Lewis M., Olsen I., Knowles J.C., Phosphate Glasses for Tissue Engineering: Part 1. Processing and Characterisation of a Ternary Based P_2O_5-CaO-Na_2O Glass System, Biomaterials 2004, 25, 491-499

[4] Franks K., Abrahams I., Knowles J.C., Development of Soluble Glasses for Biomedical Use Part I: In Vitro Solubility Measurement, J. Mater. Sci-Mater. M. 2000, 11, 609-614.

[5] Bunker B.C., Arnold G.W., Wilder J.A., Phosphate Glass Dissolution in Aqus Solutions, J. Non-Cryst. Solids 1984, 64, 291-316

[6] Ahmed I., Parsons A.J., Rudd C.D., Nazhat S.N., Knowles J.C., Guerry P., Smith M.E., Comparison of Phosphate-based Glasses in the Range $50P_2O_5$-$(50-x)CaO$-xNa_2O Prepared Using Different Precursors, Glass Technol-Part A 2008, 49, 63-72

[7] Abou Neel E.A., Salih V., Knowles J.C., Phosphate-based glasses. In: Ducheyne P. (Ed.), Comprehensive Biomaterials, 1st ed., Elsevier Science 2011

[8] Ahmed I., Collins C.A., Lewis M.P., Olsen I., Knowles J.C., Processing, Characterisation and Biocompatibility of Iron-Phosphate Glass Fibres for Tissue Engineering, Biomaterials 2004, 25, 3223-3232

[9] Navarro M., Ginebra M., Planell J.A., Cellular Response to Calcium Phosphate Glasses with Controlled Solubility, J. Biomed. Mater. Res. A 2003, 67A, 1009-1015

[10] Abou Neel E.A., Knowles J.C., Physical and Biocompatibility Studies of Novel Titanium Dioxide Doped Phosphate-based Glasses for Bone Tissue Engineering Applications, J. Mater. Sci-Mater. M. 2008, 19, 377-386

[11] Ahmed I., Lewis M., Olsen I., Knowles J.C., Phosphate Glasses for Tissue Engineering: Part 2. Processing and Characterisation of a Ternary based P_2O_5-CaO-Na_2O Glass-fibre System, Biomaterials 2004, 25,501-507

[12] Abou Neel E.A., Ahmed I., Pratten J., Nazhat S.N., Knowles J.C., Characterisation of Antibacterial Copper Releasing Degradable Phosphate Glass Fibres, Biomaterials 2005, 26,2247-2254

[13] Kobayashi H.Y.L.S., Brauer D.S., Rüssel C., Mechanical Properties of a Degradable Phosphate Glass Fibre Reinforced Polymer Composite for Internal Fracture Fixation, Mat. Sci. Eng. C-Mater. 2010, 30,1003-1007

[14] Andriano K.P., Daniels A.U., Heller J., Biocompatibility and Mechanical Properties of a Totally Absorbable Composite Material for Orthopaedic Fixation Devices, J. Appl. Biomater. 1992, 3, 197-206

[15] Felfel R.M., Ahmed I., Parsons A.J., Haque P., Walker G.S., Rudd C.D., Investigation of Crystallinity, Molecular Weight Change, and Mechanical Properties of PLA/PBG Bioresorbable Composites as Bone Fracture Fixation Plates, J. Biomater. Appl. 2012, 26,765-789

[16] Parsons A.J., Ahmed I., Haque P., Fitzpatrick B., Niazi M.I.K., Walker G.S., Rudd C.D., Phosphate Glass Fibre Composites for Bone Repair, J. Bionic Eng. 2009, 6, 318-323

[17] Furniss D., Seddon A.B., Towards Monomode Proportioned Fibreoptic Preforms by Extrusion, J. Non- Cryst. Solids, 1999, 256& 257, 232-236.

[18] Savage S.D., Miller C.A., Furniss D., Seddon A.B., Extrusion of Chalcogenide Glass Preforms and Drawing to Multimode Optical Fibers, J. Non-Cryst. Solids 2008, 354, 3418-3427

[19] Vitale-Brovarone C., Novajra G., Milanese D., Lousteau J., Knowles J.C., Novel Phosphate Glasses with Different Amounts of TiO_2 for Biomedical Applications: Dissolution Tests and Proof of Concept of Fibre Drawing, Mat. Sci. Eng. C-Mater. 2011, 31, 434-442

[20] Abou Neel E.A., Young A.M., Nazhat S.N., Knowles J.C., A Facile Synthesis Route to Prepare Microtubes from Phosphate Glass Fibres, Adv. Mater. 2007, 19, 2856-2862

[21] Mulligan A.M., Wilson M., Knowles J.C., The Effect of Increasing Copper Content in Phosphate-based Glasses on Biofilms of Streptococcus Sanguis, Biomaterials 2003, 24, 1797-1807

[22] Ahmed A.A., Ali A.A., Mahmoud D.A.R., El-Fiqi A.M., Preparation and Characterization of Antibacterial P_2O_5-CaO-Na_2O-Ag_2O Glasses, J. Biomed. Mater. Res. A 2011, 98A, 132-142

[23] Moss R.M., Structural Characteristics of Antibacterial Bioresorbable Phosphate Glass, Adv. Funct. Mater. 2008, 18, 634-639

[24] Ahmed I., Ready D., Wilson M., Knowles J.C., Antimicrobial Effect of Silver-doped Phosphate-based Glasses, J. Biomed. Mater. Res. A 2006, 79A, 618-626

[25] Ahmed I., Abou Neel E.A., Valappil S.P., Nazhat S.N., Pickup D.M., Carta D., Carroll D.L., Newport R.J., Smith M.E., Knowles J.C., The Structure and Properties of Silver-Doped Phosphate-based Glasses, J. Mater. Sci. 2007, 42, 9827-9835

[26] Wray P., 'Cotton candy' that heals?, Am. Ceram. Soc. Bull. 2011, 90, 25-28

[27] Gent A.N., Theory of the Parallel Plate Viscometer, Brit J App Phys 1960, 11, 85-87

[28] Burling L., Novel Phosphate Glasses for Bone Regeneration Applications, PhD thesis, University of Nottingham, Nottingham, UK, 2005

[29] Mairaj A.K., Feng X., Hewak D.W., Extruded Channel Waveguides in a Neodymium-doped Lead-Silicate Glass for Integrated Optic Applications, Appl. Phys. Lett. 2003, 83, 3450-3452

[30] Lee E.T.Y., Taylor E.R.M., Two-die Assembly for the Extrusion of Glasses with Dissimilar Thermal Properties for Fibre Optic Preforms, J. Mater. Process Tech. 2007, 184, 325-329

[31] Paek U.C., Kurkjian C.R., Calculation of Cooling Rate and Induced Stresses in Drawing of Optical Fibre, J. Am. Ceram. Soc. 1975, 58, 330-335

[32] Jordery S., Naftaly M., Jha A., A Review of Optical and Thermal Properties of Cadmium-Mixed Halide Glass Host for the $1.3\bar{I}1/4m$ Pr3+-doped Amplifier, J. Non-Cryst. Solids 1996, 196, 199-203

[33] Daly J.C., Fiber Optics, Taylor & Francis Ltd., Boca Raton, 1984

[34] Kurkjian C.R., Mechanical Properties of Phosphate Glasses, J. Non-Cryst. Solids. 2000, 263 & 264, 207-212

[35] Pukh V., Baikova L., Kireenko M., Tikhonova L., On the Kinetics of Crack Growth in Glass, Glass Phys. Chem 2009, 35, 560-566

[36] Orcel G., and Biswas D., Influence of Processing Parameters on the Strength of Fluoride Glass Fibers, J. Am. Ceram. Soc. 1991, 74, 1373-1377

[37] Wang J., Prasad S., Kiang K., Pattnaik R.K., Toulouse J., Jain H., Source of Optical Loss in Tellurite Glass Fibers, J. Non-Cryst.

Solids 2006, 352, 510-513

[38] Barton G.W., Law S.H., McNamara P., Phan T.N., Measurement and Control Challenges for the Specialty Optical Fibre Industry in the 21st Century, Proceedings of the 5th Asian Control Conference, (20-23 July 2004, Melbourne, Australia), 2004, 1137-1144

[39] Ahmed I., Cronin P., Abou Neel E.A., Parsons A.J., Knowles J., Rudd, C.D., Retention of Mechanical Properties and Cytocompatibility of a Phosphate-based Glass Fibre/Polylactic Acid Composite, J. Biomed. Mater. Res. B 2009, 89, 18-27

[40] Abou Neel E.A., Chrzanowski W., Georgiou G., Dalby M.J., Knowles J.C., In Vitro Biocompatibility and Mechanical Performance of Titanium Doped High Calcium Oxide Metaphosphate-Based Glasses, J. Tissue Eng. 2010,

[41] Hayden J.S., Marker III A.J., Suratwala T.I., Campbell J.H., Surface Tensile Layer Generation During Thermal Annealing of Phosphate Glass, J. Non-Cryst. Solids 2000, 263& 264, 228-239

[42] Cozien-Cazuc S., Characterisation of Resorbable Phosphate Glass Fibers, PhD thesis, University of Nottingham, Nottingham, UK, 2006

[43] Colaizzi J., Matthewson M.J., Iqbal T., Shahriari M.R., Mechanical Properties of Aluminum Fluoride Glass Fibers, Proceedings of The International Society for Optical Engineering (5-6 Sept 1991, Boston, USA), 1991, 26-33

[44] Karabulut M., Melnik E., Stefan R., Marasinghe G.K., Ray C.S., Kurkjian C.R., Day D.E., Mechanical and Structural Properties of Phosphate Glasses, J. Non-Cryst. Solids 2001, 288, 8-17

[45] Kordes E., Vogel W. and Feterowsk, Physikalisch-chemische Untersuchungen über die Eigenschaften und den Feinbau von Phosphatgläsern, Z. Elektrochem, Vol 57, Issue 4, (1953) pp 282.